



Society of Petroleum Engineers

SPE-185686-MS

Heavy Oil Recovery from Opal-CT Diatomite

J. K. Dietrich, Dietrich Corp.

Copyright 2017, Society of Petroleum Engineers

This paper was prepared for presentation at the 2017 SPE Western Regional Meeting held in Bakersfield, California, USA, 23 April 2017.

This paper was selected for presentation by an SPE program committee following review of information contained in an abstract submitted by the author(s). Contents of the paper have not been reviewed by the Society of Petroleum Engineers and are subject to correction by the author(s). The material does not necessarily reflect any position of the Society of Petroleum Engineers, its officers, or members. Electronic reproduction, distribution, or storage of any part of this paper without the written consent of the Society of Petroleum Engineers is prohibited. Permission to reproduce in print is restricted to an abstract of not more than 300 words; illustrations may not be copied. The abstract must contain conspicuous acknowledgment of SPE copyright.

Abstract

Diatomite oil reservoirs are unconventional. They hold billions of barrels of oil in a tight rock matrix with unusual physical properties, and contain a stress-sensitive natural fracture system that introduces a strong permeability anisotropy during fluid injection. Perhaps the most unusual feature of diatomite is geochemical in nature. Diatomite undergoes a silica-phase reordering and transformation as temperature is raised, whereby amorphous Opal-A is converted to a more ordered Opal-A' and more dense, crystalline Opal-CT. The injection of steam accelerates this naturally occurring process and leads to rapid densification and compaction and an irreversible loss of permeability.

Nearly all of the field projects have been installed in Opal-A. Opal-CT is less permeable and this is the primary reason its development has been deferred. Although Opal-CT is less permeable under initial reservoir conditions, its stress and temperature-dependent compaction coefficients are much lower than those of Opal-A. As steam injection elevates reservoir temperature over time, the difference in permeability of Opal-A and Opal-CT is expected to narrow. It is chiefly for this reason that Opal-CT may hold more promise than currently supposed.

The Opal-A field projects have demonstrated that closely spaced rows of wells are necessary for efficient oil recovery by water or steam injection. What is now called ultra-tight well spacing with rows of hydraulically fractured injectors and producers spaced only 35 to 45 feet apart was shown via numerical modeling more than 20 years ago to be necessary for maximizing oil recovery. That early modeling made use of laboratory determined rock and fluid properties and included the effects of thermally induced compaction. Following tuning of the early models using hydraulically fractured cyclic steam response, they were used to estimate ultimate recovery and thermal efficiency for steam injection into diatomite containing heavy oil. Given Opal-CT and ultra-tight well spacing, a combined cyclic steam and steamflood process was shown to be capable of ultimately recovering about 40% of the original oil-in-place, with a CSOR of 3 to 4 barrels of CWE steam per barrel of oil.

Introduction

The California Diatomite Thermal Study Project (CDTSP) was a privately funded consortium research project undertaken from 1991 to 1993. The goal of the project was to design a thermal oil recovery process for the recovery of heavy oil from diatomite which might warrant field pilot testing. The technical approach involved laboratory determination of diatomite rock and fluid properties, followed by scale-up to the field

using thermal reservoir simulation. Study sites were selected by the participating companies to include Opal-A and Opal-CT diatomite accumulations at Cymric, North Midway Sunset and South Belridge in the San Joaquin Valley of California. Core material and fluid samples representing 12 and 18° API oils were shipped from these sites to the laboratories chosen to perform the work. The laboratory rock and fluid property data have previously been published ([Dietrich and Scott 2007](#), and [Dietrich 2010](#)).

The project provided an understanding of the encouraging potential for recovering oil from diatomite through application of the cyclic steam and steamflooding processes using hydraulically fractured vertical wells. It highlighted (1) the benefits that accrue from flowing rather than pumping the production wells, and (2) the need for what is now called ultra-tight well spacing. Learned more than 20 years ago, these two key features of diatomite development are described in this paper. Early claims of their importance are confirmed by published results from field pilot projects ([Murer and McClenen et al. 2000](#), [Allan and Gold et al. 2010](#), and [Elias and Wilson et al. 2010](#)).

Stress-Sensitive Fracture System

Numerically computed heating patterns that result from a conceptual model of fluid movement through a stress-sensitive natural fracture system are at the heart of what is offered here about diatomite thermal oil recovery potential. The conceptual model is a product of extensive diatomite waterflooding experience gained while participating in the early development of the Belridge oil field.

Natural Fractures. Open natural fractures are often found in the clean Opal-A rock types "A" and "B" which contain little terrigenous material; dirty Opal-A (rock type "C") and the mudstones and siltstones are found to rarely contain natural fractures ([Dietrich and Scott 2007](#)). The natural fractures are vertically oriented and only a few inches in height. Evaluation of oriented core material and response to fluid injection further indicate that the natural fractures strike parallel to the maximum horizontal principal stress direction as indicated by the orientation of the hydraulically induced fractures. The trend of the natural fracture system is unidirectional in nature; orthogonal natural fractures are typically rare or absent. [Lorenz et al. \(1989\)](#) provide a plausible explanation for the absence of an orthogonal set of natural fractures: that is, in low-permeability reservoirs found in tectonically inactive areas, few high-angle, orthogonal fractures exist because natural fractures in this type of environment are created by high pore pressures and relatively low differential horizontal (tectonic) stresses, rather than by significant structural deformation.

[McGuire \(1983\)](#) earlier had postulated that overpressuring created a set of unidirectional microfractures oriented perpendicular to the axis of least-compressive stress in the diatomite at Lost Hills. A possible source of the increase in pore pressure was offered to be the compaction, densification, and porosity loss which result from the reordering and transformation of Opal-A to Opal-A' and Opal-CT ([Ross and Vega et al. 2016](#)).

Elastic properties derived from sonic and density logs indicate that the least horizontal principal stress is likely to be initially less in the rich diatomite layers. Given both injection and compaction as mechanisms for increasing pore pressure and canceling effective stress, the layers subjected to the smallest stress at the outset will be the layers to first reach an effective tensile stress and crack. Hence, with this type of fracture generation model in mind, we expect that fluids will move in the orthogonal, or off-trend, direction preferentially through relatively thin layers of rich Opal-A rock types "A" and "B", containing vertically oriented tension cracks or joints that are *newly created* in response to increasing pore pressure.

Permeability Anisotropy. Pressure transient testing in diatomite reveals that the natural fracture system is stress-sensitive ([Chase and Dietrich 1988](#)). Fracture conductivity increases because of dilation under fluid injection, and it decreases to the matrix level during pressure drawdown near production wells. When modeling either primary depletion or laboratory flow experiments, the natural fracture system will be closed or absent and only matrix flow needs to be considered. In this case, permeability can be treated isotropically and related to strain-dependent porosity. The modeling of diatomite fluid-injection processes requires a

different procedure, one in which the effect of the natural fractures and tension joints is included through the use of a permeability anisotropy that is stress-dependent. Where the effective stress is greater than the initial in-situ level (that is, near production wells where the natural fractures are expected to be closed), the permeability distribution is treated as isotropic. However, where the effective stress is less than the initial level (that is, near injection wells where the unidirectional natural fractures and joints are open and dilated), the permeability distribution is treated as strongly anisotropic; it will be approximately equal to the matrix level in the orthogonal, or off-trend, direction and equal to that level needed to reproduce the measured steam injectivity in the on-trend direction.

Cyclic Steam Potential

The potential for recovering oil from diatomite through application of the cyclic steam process was studied for both Opal-CT and Opal-A. The majority of effort was used to evaluate two cyclically steamed wells completed in very dissimilar diatomite rock types (Table 1), both containing a 12°API oil (Oil "A" in Tables 2, 3 and 4). This approach was taken to determine if the thermal simulator used in the study (Chase and Dietrich 1989, Dietrich and Norman 2003, and Dietrich and Scott 2007) could be successfully tuned to match the observed, widely differing field performance. Long-term cyclic steam response was evaluated for Opal-CT conditions at Cymric; Opal-A response was studied at South Belridge.

Table 1—Model Rock Properties

| Table 1 – Model Rock Properties | | |
|---|---------------------------------|---|
| Parameter | Cymric Opal-CT Rock Type "D" | South Belridge Opal-A Rock Type "C" |
| Effective porosity, % bulk vol. | 48.5 | 32 to 42 |
| Matrix absolute liquid permeability, md | 1.5 | 5.0 |
| Stress-dependent compaction coefficient, psi^{-1} | 20 E-06 | 150 E-06 to 275 E-06 |
| Temperature-dependent compaction coefficient at $T < 215^{\circ}\text{F}$, $^{\circ}\text{F}^{-1}$ | 175 E-06 to 300 E-06 | 500 E-06 to 750 E-06 |
| Temperature-dependent compaction coefficient at $T > 215^{\circ}\text{F}$, $^{\circ}\text{F}^{-1}$ | -- | 100 E-06 to 200 E-06 |
| Matrix endpoint effective water permeability, md | 0.1 | 0.4 |
| Average initial effective oil saturation, % pore vol. | 56 | 42 |
| Thermal conductivity, Btu / ft · day · $^{\circ}\text{F}$ | 14.0 | 14.0 |
| Volumetric heat capacity adjusted for absent non-pay, Btu / $\text{ft}^3 \cdot ^{\circ}\text{F}$ | 44.0 | 32.5 |
| Residual oil saturation to water displacement at 330°F, % PV | 19.5 | 19 |
| Residual oil saturation to steam displacement at 330°F, % PV | 18 | 17 |
| Residual oil saturation to steam displacement at 550°F, % PV | 12.5 | 8.0 |
| Exponent gamma (γ) in porosity-dependent permeability equation, $k / k_0 = (\phi / \phi_0)^{\gamma}$ | 9.55 | 11.85 |

Table 2—Measured Oil Density Oil "A" Used in Model

| Temperature | | Oil density, kg / m^3 oil A | Oil density, kg / m^3 oil B |
|-------------|-----|---|---|
| °F | °C | | |
| 91 | 33 | -- | 927.2 |
| 110 | 43 | 957.3 | -- |
| 176 | 80 | 932.1 | 899.5 |
| 330 | 165 | 880.9 | 849.0 |
| 392 | 200 | 860.1 | 828.5 |
| 550 | 288 | 804.2 | 777.2 |

Table 3—Measured Oil Viscosity Oil "A" Used in Model

| Temperature °F °C | Oil "A" Dead-oil* viscosity, cp | Oil "A" Live-oil** viscosity, cp | Oil "B" Dead-oil* viscosity, cp | Oil "B" Live-oil** viscosity, cp |
|-------------------------|---------------------------------|----------------------------------|---------------------------------|----------------------------------|
| 91 33 | -- | -- | 218 | 109.5 |
| 110 43 | 2954 | 1742.2 | -- | -- |
| 176 80 | 181.1 | 152.0 | 20.9 | 15.0 |
| 330 165 | 8.9 | 7.4 | 2.4 | 1.8 |
| 392 200 | 4.9 | 4.6 | 1.5 | 1.2 |
| 550 288 | 2.20 | 1.95 | 0.68 | 0.64 |

*Oil "A" is 12.3 °API, Oil "B" is 17.8 °API

**Live-oil "A" and "B" at 1300 psi, Oil "A" recombined gas is 30.0 scf / bbl at 110°F, Oil "B" recombined gas is 38.2 scf / bbl at 91°F

Table 4—Measured Live Oil Thermal Expansivity Oil "A" Used in Model

| Temperature | | | Temperature | | Oil expansivity m ³ / m ³ / °C oil A | oil expansivity m ³ / m ³ / °C oil B |
|-------------|----|----|-------------|-----|---|--|
| °F | °C | | °F | °C | | |
| 91 | 33 | to | 176 | 80 | -- | 0.000651 |
| 110 | 43 | to | 176 | 80 | 0.000623 | -- |
| 176 | 80 | to | 330 | 165 | 0.000680 | 0.000698 |

Opal-CT

The Cymric well chosen for evaluation was completed during 1990. It was hydraulically fractured and propped with about 246,000 pounds of sand over the interval 1512-1754 feet, shown in the calculated log plots of Fig. 1, where the track headings are defined below under **Nomenclature**. The average N/G ratio of the completion interval is about 0.8; the oil concentration within the net pay varies from 800 to 1600 bbl/ac-ft and averages 1420 bbl/ac-ft. At the time of this study, the operator had completed 2 steam cycles in this well. A volume of 9,590 barrels of CWE steam was injected during a 15-day period to start the first cycle. Tubing-head injection pressure was reported as 694 psi and the downhole steam quality was estimated to have been about 47%. These two cycles were matched with the simulator, primarily by adjusting the length and conductivity of the propped fracture (Table 5), while injecting and producing under limiting bottom-hole pressure controls *without constraint of the model fluid rates* (Table 6). The tuned simulator was then allowed to run, assuming an operating strategy involving small steam slugs followed by flowback without pumping, until an uneconomic SOR was reached after 28 cycles (Fig. 2). In these simulations, the minimum flowing bottom-hole pressure was set at 200 psi, and the flowback period was taken at about 60 days. The following results are based upon injecting a series of 4,000 barrel CWE steam slugs at 925 Btu/lb steam into 200 feet of Opal-CT with an average initial effective oil saturation of 56%; all of the CSOR numbers given in this paper are model numbers that have been normalized to reflect 1,000 Btu/lb steam for consistency:

- the cyclic steam process was shown to be capable of recovering about 13% of the oil initially in-place within a drainage area of ½ acre during 5-½ years at a CSOR of 4.0 bbl/bbl

- wells drilled on $\frac{3}{4}$ acre spacing or less will experience significant pressure interference during cyclic steaming operations (Figs. 3 through 6)
- at the end of the cyclic steam process, the maximum thermally stimulated acreage surrounding the well will only be $\sim \frac{1}{4}$ acre (Fig. 7)

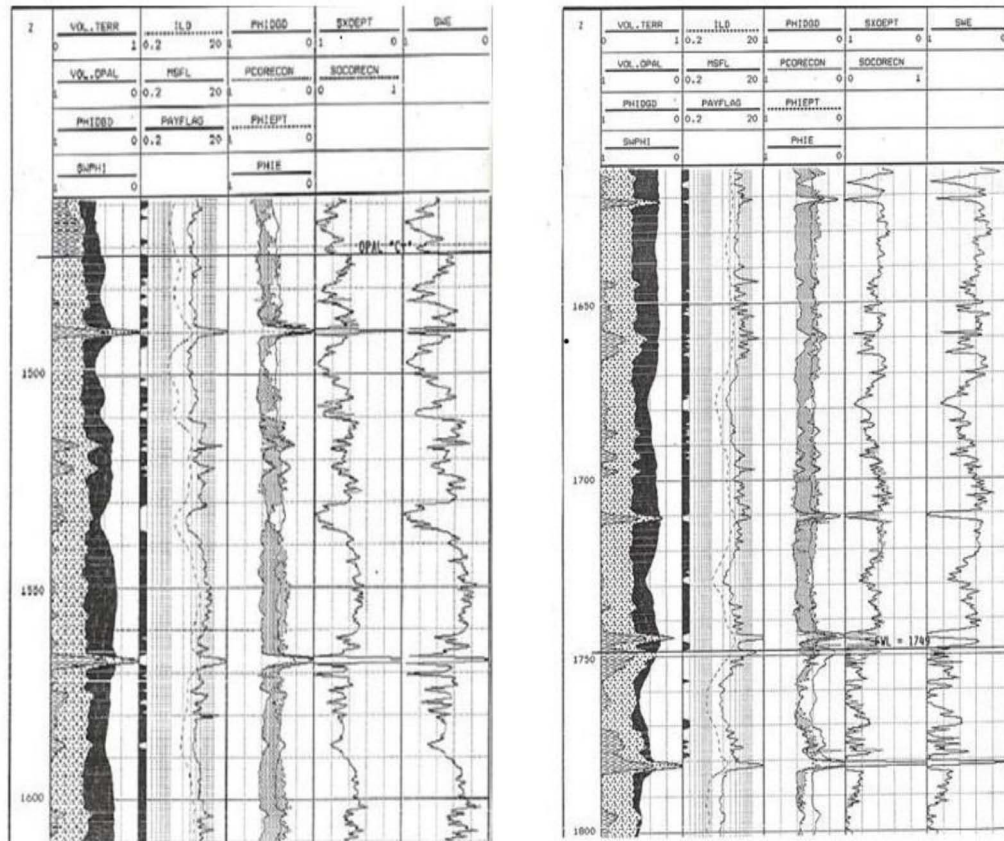


Figure 1—Cymric Opal-CT log response

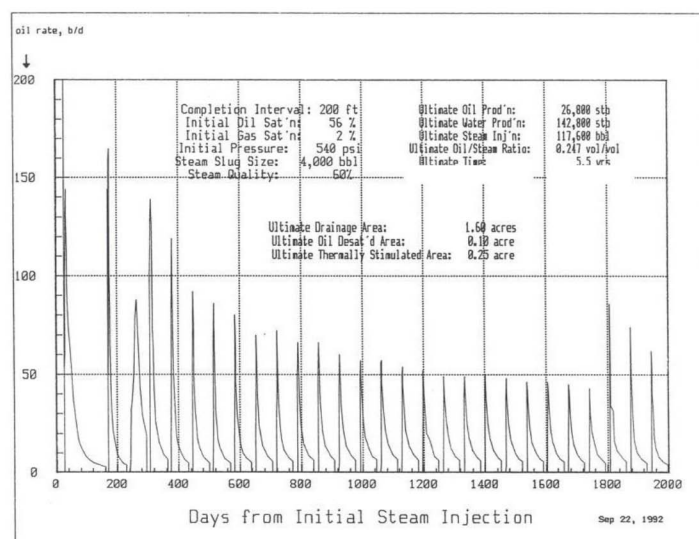


Figure 2—Cymric Opal-CT model cycle oil rates

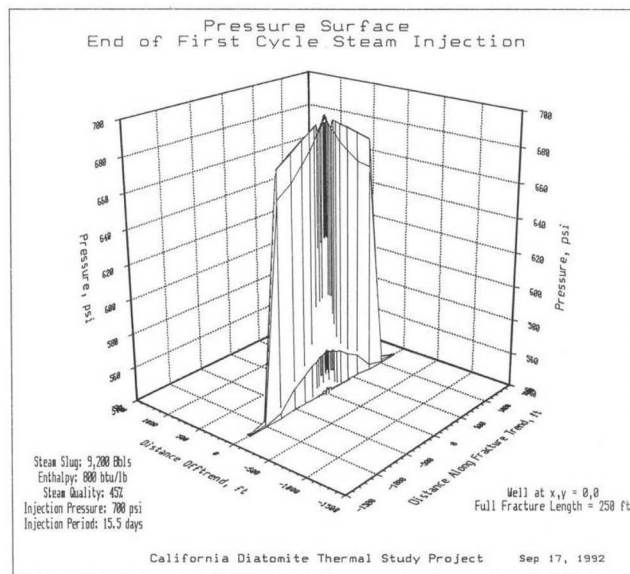


Figure 3—Cymric Opal-CT well -pressure in propped hydraulic fracture at era of 1st cycle steam injection

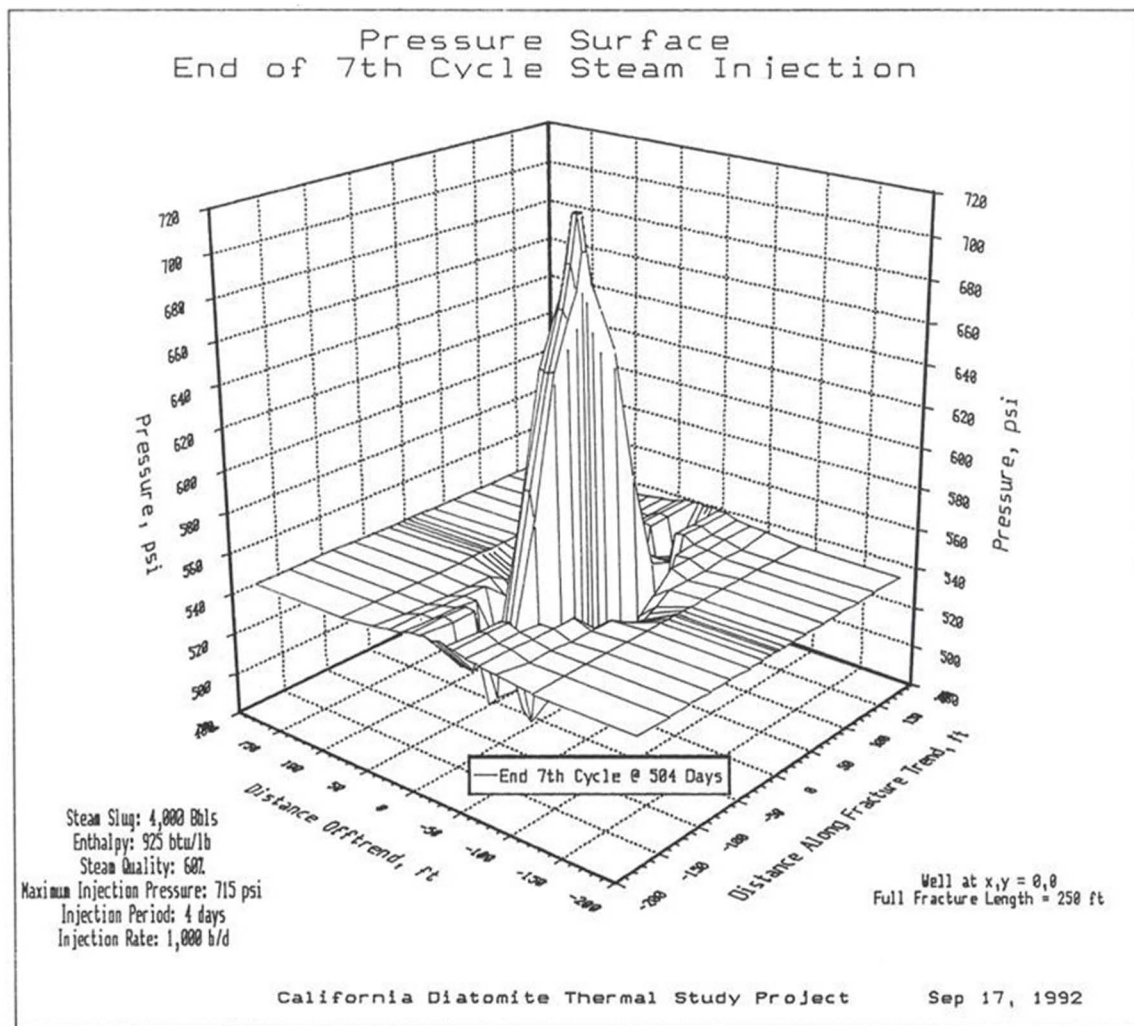


Figure 4—Cymric Opal-CT well - pressure in propped hydraulic fracture at end of 7th cycle steam injection

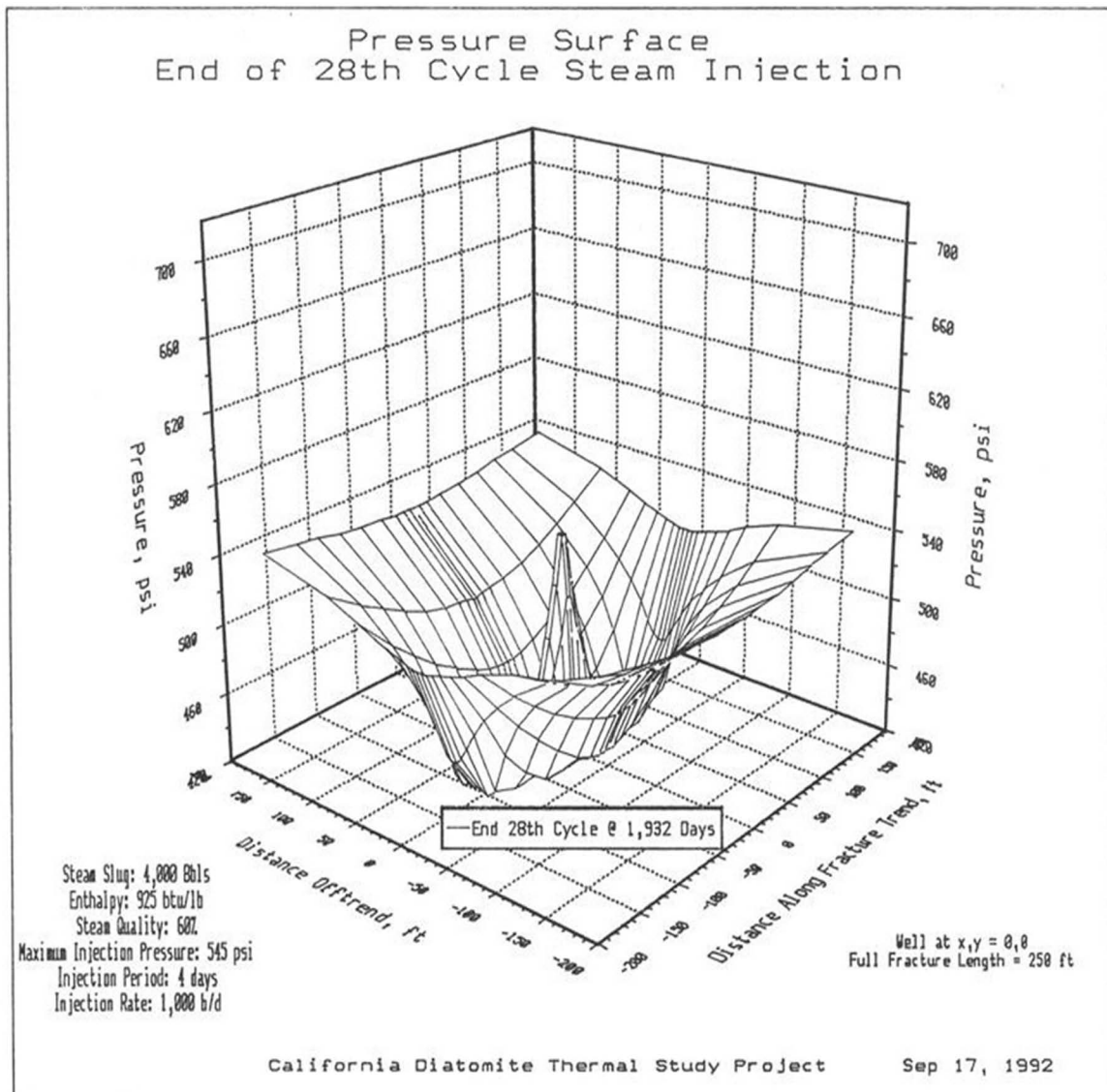


Figure 5—Cymric Opal-CT well - pressure in propped hydraulic fracture at end of 28th cycle steam injection

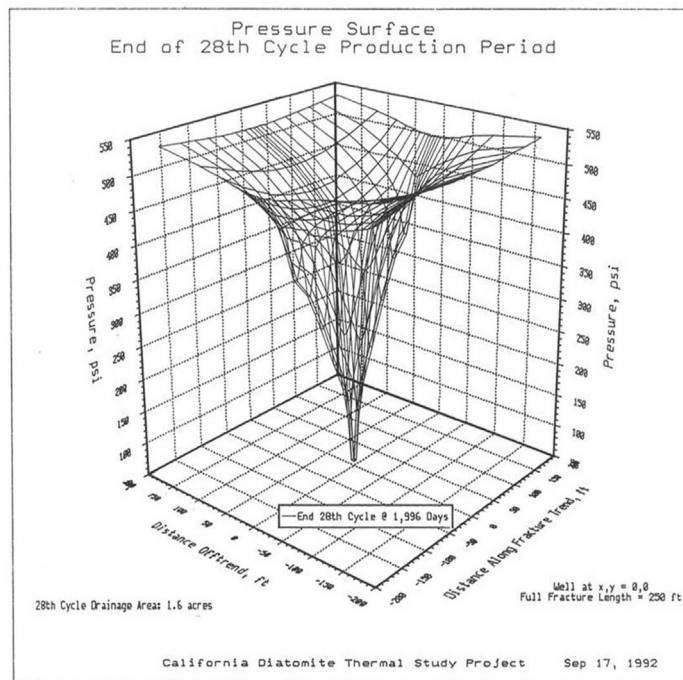


Figure 6—Cymric Opal-CT well - pressure in and near propped hydraulic fracture al end of 28th cycle production period

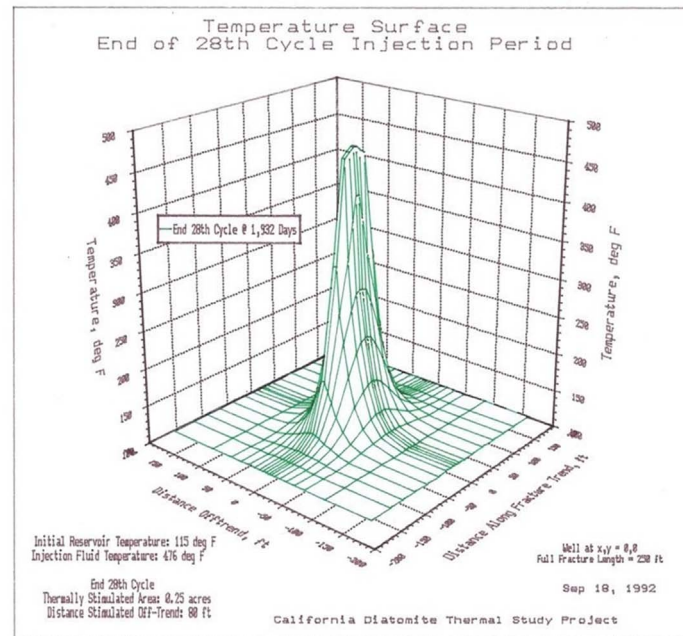


Figure 7—Cymric Opal-CT well - temperature in and near propped hydraulic fracture at end of 28th cycle steam injection

Table 5—Model Hydraulically-Induced Fracture Properties

| Parameter | Opal-CT Rock Type "D" 1st Cycle Propped Fracture | Opal-A Rock Type "C" 1st Cycle Steam Fracture |
|---|---|--|
| Fracture half length, ft | 125 | 500 |
| Fracture conductivity during injection, md-ft | 10,000 | 50,000 |
| Fracture conductivity during production, md-ft | 200 | 50,000 |
| Exponent gamma (γ) in porosity-dependent permeability equation, $k / k_0 = (\phi / \phi_0)^\gamma$ | 2 | 8 |

Table 6—Cymric Opal-CT Well 1st Steam Cycle - Actual vs Model

| Parameter | Cycle 1 Actual | Cycle 1 Model |
|---|-------------------|------------------|
| Steam injected, bbl CWE | 9,590 | 9,162 |
| Estimated bottom-hole steam quality, % | 45 | 45 |
| Estimated bottom-hole steam enthalpy, Btu/lb | 800 | 800 |
| Maximum surface injection pressure, psi | 694 | 700 |
| Injection duration, days | 15 | 15-½ |
| Average steam injection rate, bbl CWE/day | 640 | 591 |
| Soak duration, days | 11 | 11 |
| Initial gross liquid rate, STB/D | 350 | 280 |
| Initial oil rate, STB/D | 330 | 230 |
| Estimated bottom-hole operating pressure, psi | 25 | 25 |
| Initial instantaneous water cut, % | 6 | 18 |
| Cumulative gross liquid production, STB | 10,912 | 9,698 |
| Cumulative oil production, STB | 2,940 | 3,185 |
| Cumulative water cut, % | 73 | 67 |
| Production period, days | 134 | 134 |

The statement of 13% oil recovery efficiency requires clarification. First, oil-in-place for this calculation was taken as the volume of oil within an area of $\frac{1}{2}$ acre. This area represents the acreage affected by pressure depletion after 14 cycles. Since each of the 28 cycles did not stimulate the full 1-½-acre ultimate drainage area, it seems reasonable to use the stimulated acreage after, say, half the number of cycles as the basis for calculating recovery efficiency. And secondly, this is the recovery efficiency which may ultimately be realized in that portion of the overall thickness of pay into which an operator can successfully inject steam.

Reservoir Compaction. It was determined that compaction adds little to the overall recovery mechanism for the cyclic steam process in Opal-CT diatomite. The 28 steam cycles were re-simulated, after removing all of the laboratory measured compaction data including the non-linear strain, creep and porosity-dependent permeability data. Surprisingly, overall oil and liquid recoveries were within 2% of the result achieved when compaction was fully active. Fig. 8 indicates that a vapor phase forms near the production well and persists throughout the production period. Steam occurs nearest the well, and this is surrounded by hydrocarbon gas which has been driven out of the oil by the elevated temperature. The high compressibility of this persistent vapor phase provides the dominant source of reservoir energy when cyclic steaming Opal-CT. The amount of volatile hydrocarbon component which will exist in either the oil or vapor phase, depending upon the temperature and pressure, has been experimentally determined in this project. K-values for the 12° API oil have been entered into the simulator for the cyclic steam simulations reported here.

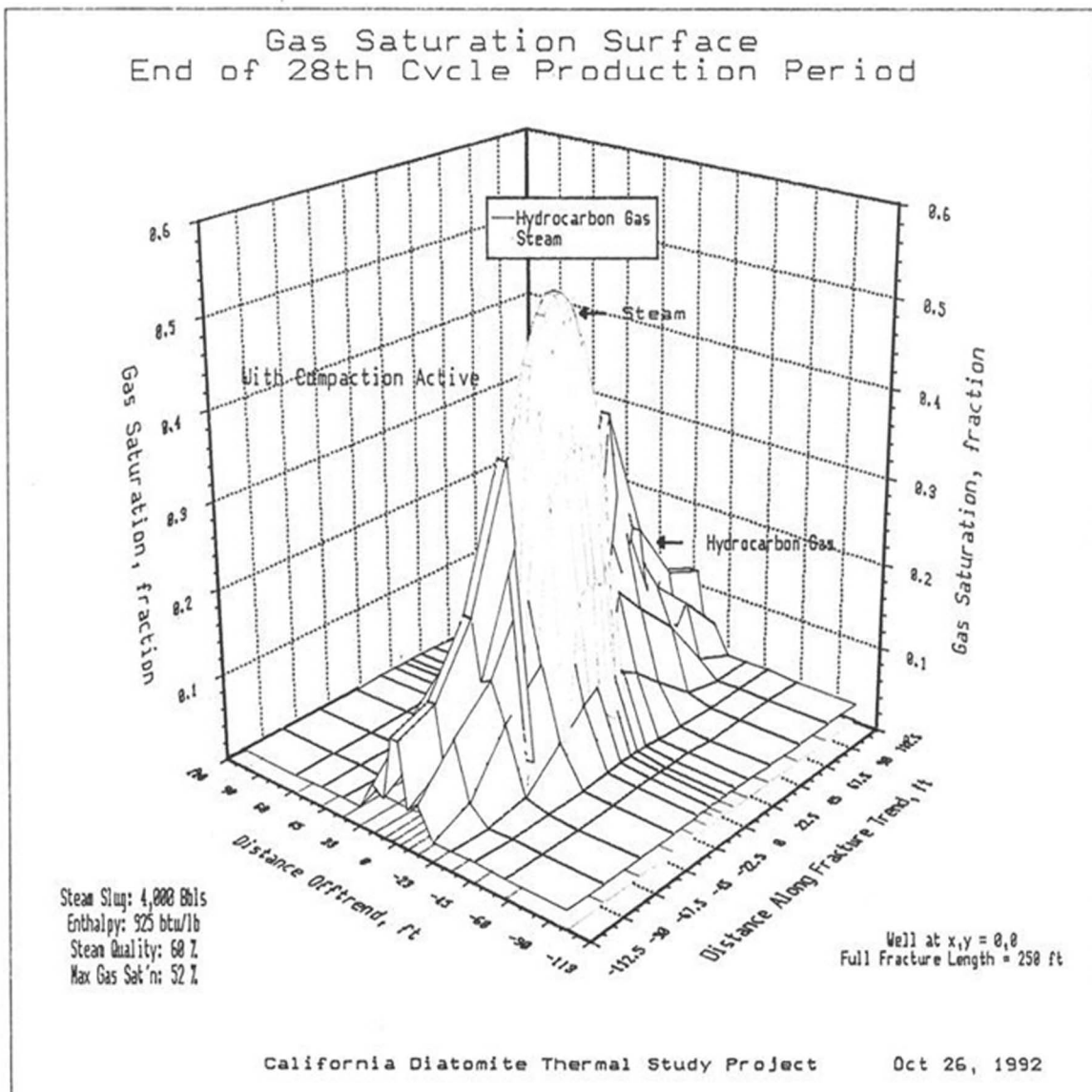


Figure 8—Cymric Opal-CT well - steam and hydrocarbon gas saturation in vapor phase in and near propped hydraulic fracture at end of 26th cycle production period

In the case where compaction was active, the compacted reservoir volume after 28 cycles of steam stimulation was negligible. There was no growth of the compaction cone surrounding the well after the initial steam cycle for the case of repetitive 4,000 barrel CWE steam slugs. The weak role of compaction demonstrated in this case is a result of flowing rather than pumping the stimulated wells. This means that given Opal-CT rock type "D" non-linear strain data (Dietrich and Scott 2007), the effective stress did not reach levels under the imposed minimum 200 psi bottom-hole flowing conditions which could significantly reduce permeability.

Steam Slug Size. Steam slug size was increased from 4,000 to 10,000 and then to 16,000 barrels CWE in two repeats of the earlier prediction work for the Cymric Opal-CT well. The soak period was set at 4 days in the original 4,000 barrel CWE slug case; this was changed to 10 days for the 10,000 barrel slug run and 16 days for the 16,000 barrel case. The flowing periods were set at 2, 3 and 4-½ months for these cases, which resulted in a flowing rate of about 8 BOPD at the end of each cycle. All other variables were unchanged, including the steam quality of 70%, the maximum steam injection pressure of 900 psi and the minimum bottom-hole flowing pressure of 200 psi. The use of 10,000 barrel steam slugs was shown to be capable of

increasing oil recovery by about 30% after 5 years of operations, as compared to the 4,000 barrel steam slug case. The 16,000 barrel case was terminated early when it was realized that as long as 3-½ months were required to inject and soak for this size of stimulation.

When using the smaller steam slugs, more total steam usage (or heat usage since the enthalpy of the injected steam is set at 925 Btu/lb in all of these runs) is required to recover the same volume of oil as recovered when using the larger steam slugs. More of the reservoir, particularly in the on-trend direction, has been heated to elevated temperature in the 10,000 barrel slug case as compared to the 4,000 barrel slug case, given the same amount of heat injection. Cycle oil-cuts are higher for the larger steam slug size as a result of this improved heating. The improved heating is caused by lower heat production losses with the larger slug size. At the equivalent point in time when the same amount of heat has been injected, 43% of the injected heat was produced back for the 10,000 barrel slug case, whereas 57% of the injected heat was produced back for the 4,000 barrel slug case. The flowback period is a higher fraction of the total cycle time for the small versus larger slug cases.

Opal-A

The South Belridge well selected for study was completed during 1991. It was perforated from 965-1115 feet (Fig. 9) in the Etchegoin and Belridge Diatomite interval and is the pilot test well described comprehensively by Murer et al. (2000). The average N/G ratio of this completion interval is about 0.7; the oil concentration within the net pay varies from 830 to 1300 bbl/ac-ft and averages 1060 bbl/ac-ft. At the time of the project, the operator had completed 5 steam cycles. The well was steamed and produced during the first 4 cycles without hydraulically fracturing and propping the completion interval. Between the fourth and fifth cycles, the well was fraced and propped with 180,600 pounds of sand. The operator injected a low-quality 8,081 barrel steam slug to start the cyclic process. This was followed by steam slugs of 8,013, 15,150, 4,000 and 7,500 barrels on the next 4 cycles; in each case, the down-hole quality was increased to about 70% at injection pressures of approximately 1,050 psig. This carefully planned sequence of slug sizes afforded an excellent opportunity to tune the simulator against real field response prior to using it to predict ultimate cyclic steam performance.

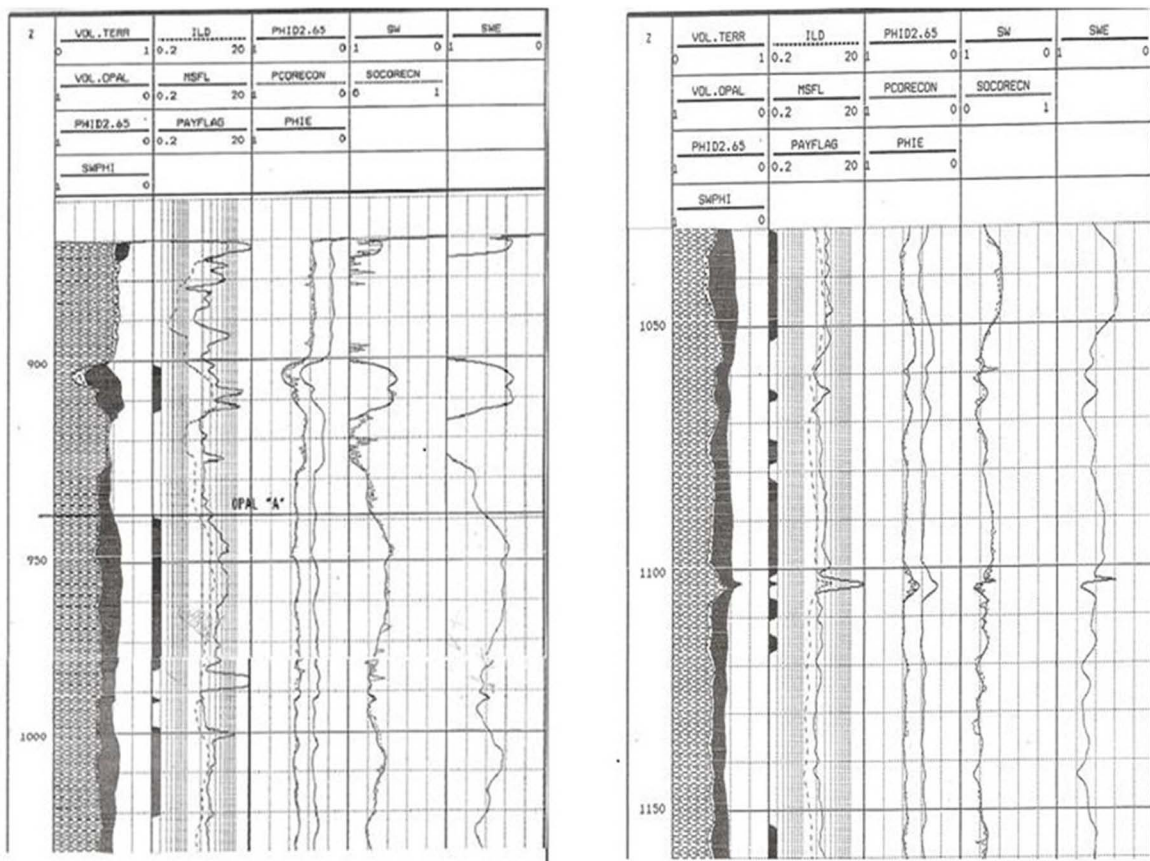


Figure 9—South Belridge Opal-A log response

The simulator was shown to be capable of reproducing the trend of high early oil production followed by a period of very low oil rates during the first 5 steam cycles (Figs. 10 through 15). It was not possible to reproduce the early high oil rates during the first 4 cycles without allowing a steam-induced fracture to close gradually over time. The procedure used in this regard was to divide the production period into two stages: a flowing stage in which the steam-induced fracture was open, and a pumping stage in which it was closed. The operator reported the time when pumping began for each cycle. The minimum bottom-hole flowing pressure was set in the model at 300 to 420 psi during the flow period, and between 15 and 25 psi during the pumping period. The simulator was restarted at the end of the fifth cycle and several additional cycles were simulated (Figs. 16 through 18). Performance predictions were not continued beyond cycle eight, because of uneconomic cycle oil recovery. These results are based specifically upon injecting a series of 8,000 barrel steam slugs at 1,000 Btu/lb steam into 150 feet of Opal-A pay with a pore-volume weighted average initial effective oil saturation of 42.5%:

- the cyclic steam process was shown to be capable of recovering about 10% of the oil initially in-place within a drainage area of $\frac{1}{2}$ acre during $2\frac{3}{4}$ years at a CSOR of 7.1 bbl/bbl
- wells drilled on $\sim \frac{1}{2}$ acre spacing or less will experience significant pressure interference during cyclic steaming operations (Figs. 19 and 20)
- at the end of the cyclic steam process, the maximum thermally stimulated acreage surrounding the well will only be $\sim \frac{1}{2}$ acre (Fig. 21)

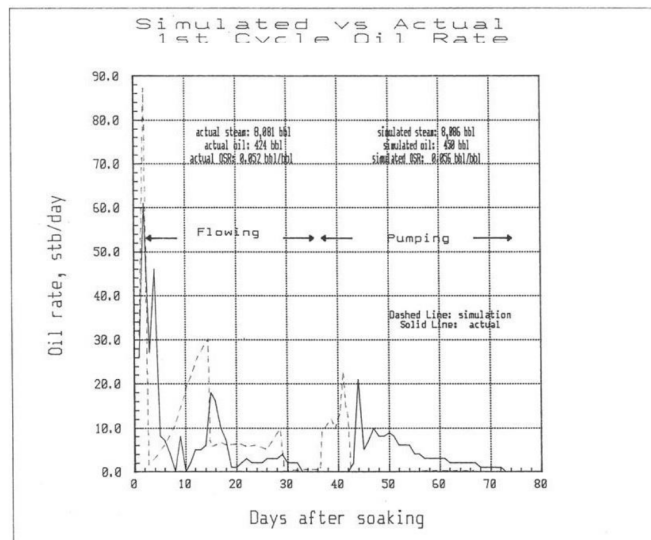


Figure 10—South Belridge Opal-A well - model versus field 1st cycle Oil rates

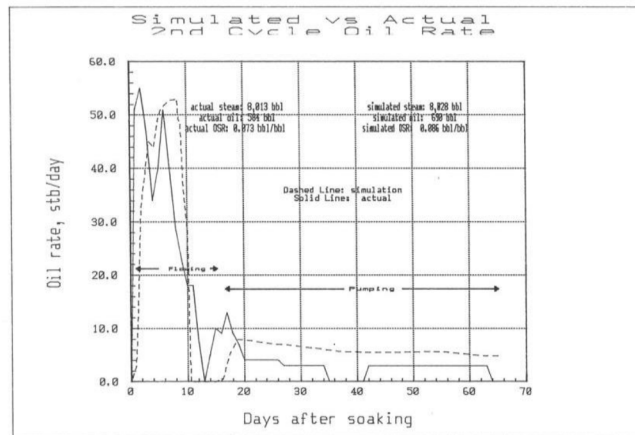


Figure 11—South Belridge Opoi-A well -model versus field 2nd cycle oil rates

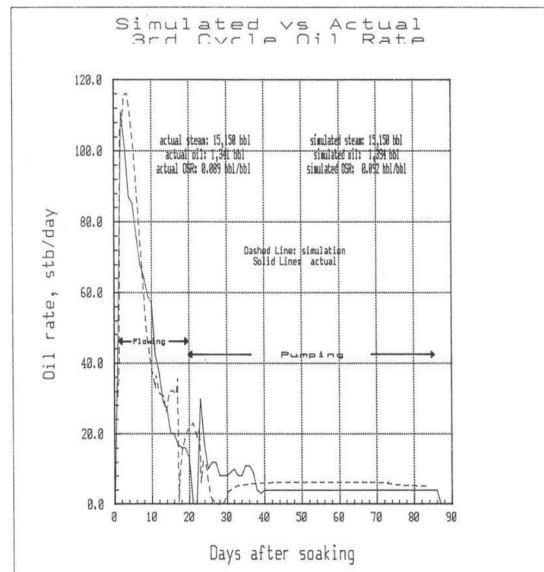


Figure 12—South Belridge Opal-A well - model versus field 3rd cycle oil rates

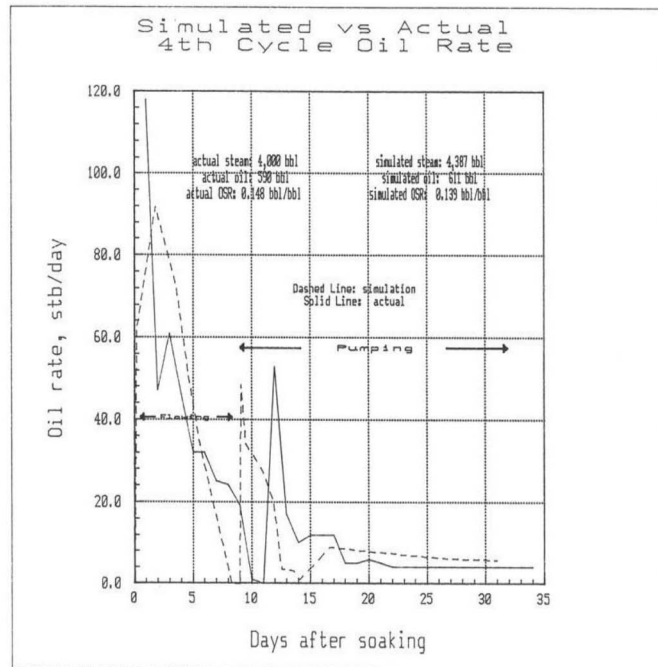


Figure 13—South Belridge Opal-A well - model versus field 4th cycle oil rates

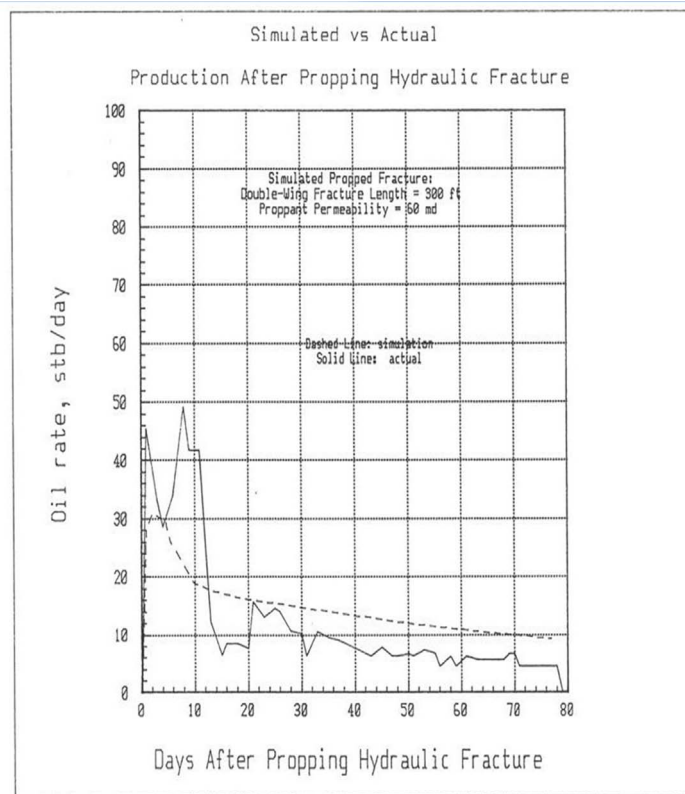


Figure 14—South Belridge Opal-A well - mode versus field oil rate after placement of propped hydraulic fracture

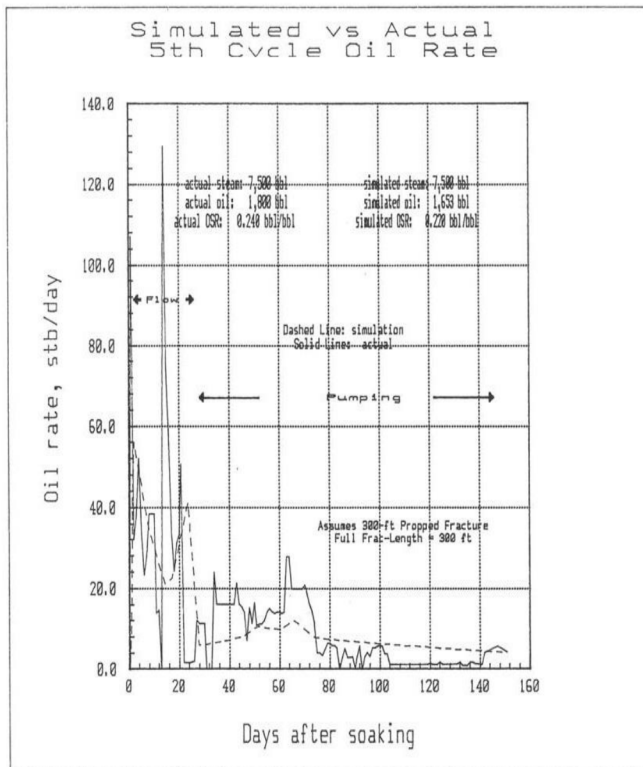


Figure 15—South Belridge Opal-A well - model versus field 5th cycle oil rates

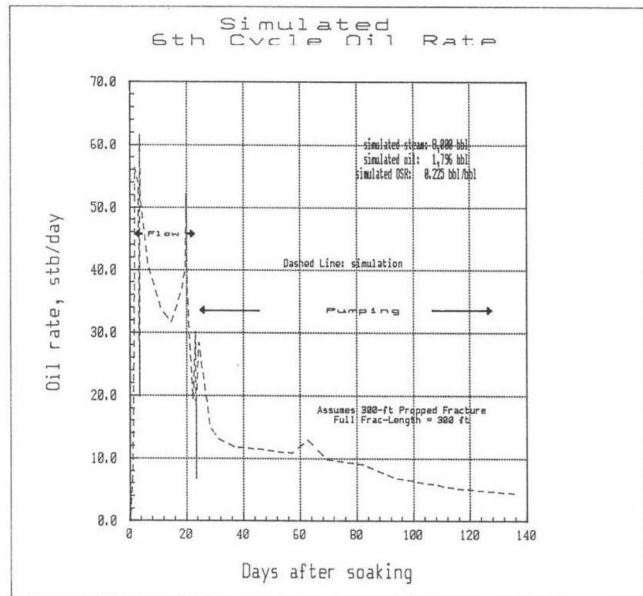


Figure 16—South Belridge Opal-A well - model 6th cycle oil rate

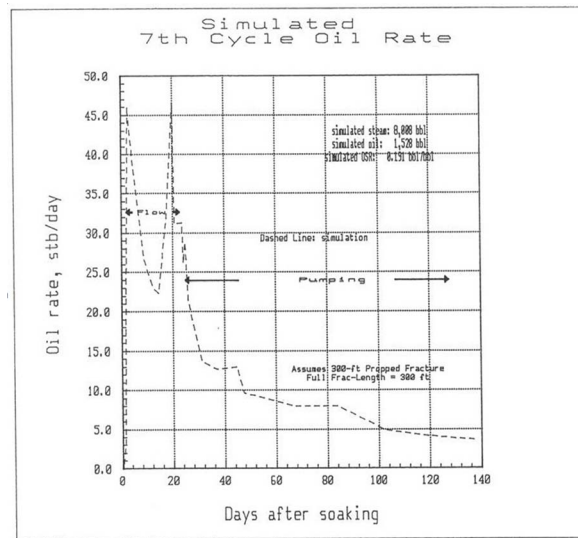


Figure 17—South Belridge Opal-A well - model 7th cycle oil rate

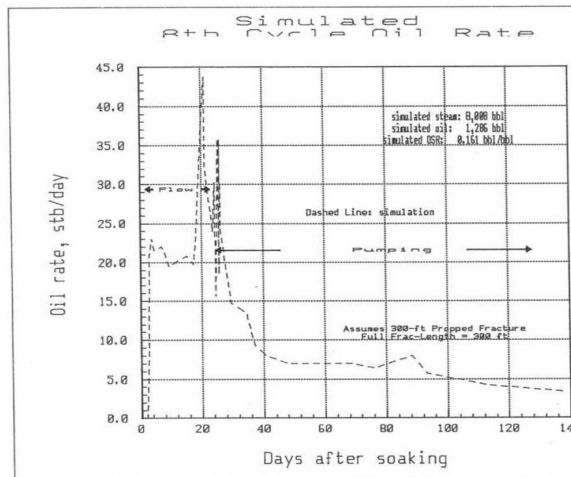


Figure 18—South Belridge Opal-A well - model 8th cycle oil rate

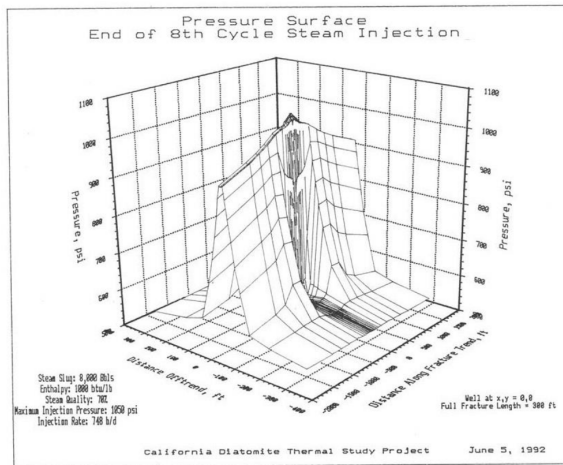


Figure 19—South Belridge Opal-A well - pressure In and near propped hydraulic fracture at end of 8th cycle steam injection

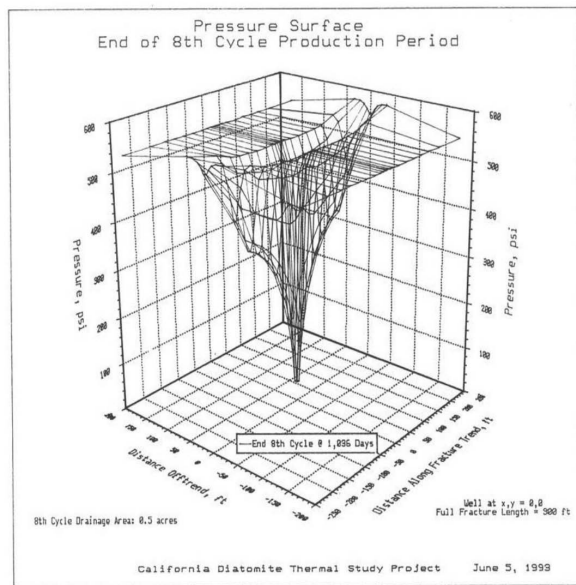


Figure 20—South Belridge Opal-A well - pressure in and near propped hydraulic fracture at end of 8th cycle production period

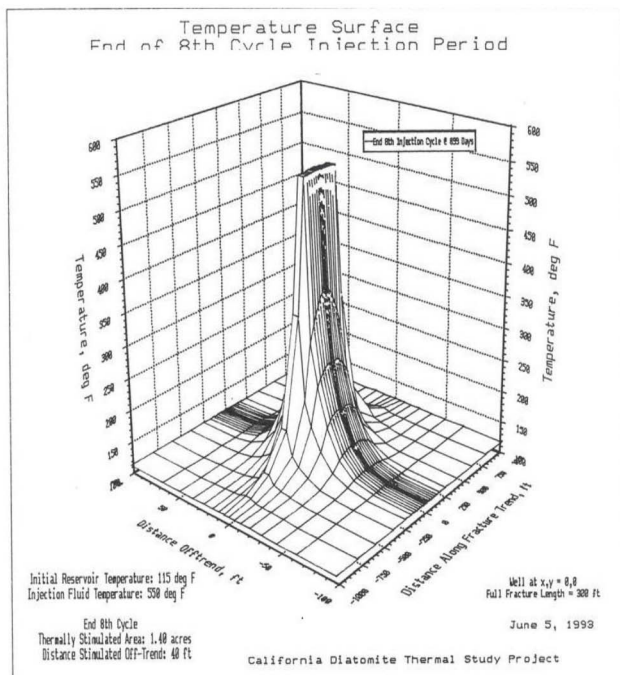


Figure 21—South Belridge Opal-A well - temperature in and near propped hydraulic fracture at end of 8th cycle steam injection

Discussion of Results

The poor cyclic steam performance of the Opal-A well at South Belridge, relative to that demonstrated for the Opal-CT well at Cymric, requires an explanation. Three important reservoir parameters are significantly different at these two sites: the SoPhi product, thermal diffusivity and the experimentally derived non-linear strain function. Oil recovery efficiency and thermal efficiency are directly proportional to the product of effective oil saturation and effective porosity (SoPhi), where effective porosity is the difference between total porosity and microporosity and effective oil saturation is the oil saturation within the effective pore system. The average SoPhi product is about $(0.56)(0.486) = 0.272$ for the Opal-CT site and only about $(0.423)(0.35) = 0.148$ for the Opal-A site selected for the project.

In a substance of high thermal diffusivity, λ , heat moves rapidly through it because the substance conducts heat quickly relative to its volumetric heat capacity, or "thermal bulk". In most liquid-saturated sand or sandstone reservoirs, λ is approximately 0.04 ft²/hr. The λ of liquid-saturated Opal-CT rock type "D" is also approximately 0.04 ft²/hr, a value that is about twice that of liquid-saturated Opal-A (Dietrich and Scott 2007). Thermal inertia is therefore expected to be much higher in Opal-A than in Opal-CT. The postulate of Elias and Powell et al. (2015), "... (Opal-A) diatomite has an inherent low rate of heat absorption compared to other oil bearing rocks ..." is consistent with the experimental results for the λ of Opal-A.

Regarding the non-linear strain function, much more strain or compaction was measured for a given temperature and change in effective stress for rock type "C" found at the Opal-A site than for rock type "D" found at the Opal-CT site (Fig. 22). Pumping conditions imposed for the South Belridge Opal-A well led to large changes in effective stress and, therefore, to high strain and loss of permeability at elevated temperatures. The permeability loss would be less significant for the Opal-A example if flowback conditions were used, as simulated for the Cymric Opal-CT well. It is the significant loss of permeability at elevated temperature in Opal-A that slows the movement of fluids in the off-trend direction and leads to much different pressure distributions than found when modeling Opal-CT (compare Figs. 5 and 6 with Figs. 19 and 20). The lack of pressure increase shown in the off-trend direction nearest the Opal-A wellbore after 8 steam cycles (Fig. 19) is due to degraded permeability, caused by an increase in effective stress and high temperature near the wellbore (Fig. 21). These computed results are consistent with a reported decrease in flow capacity calculated during *later* steam cycles in the Orcutt field of California (Elias and Medizade 2013), where an Opal-A rock type "C" is found.

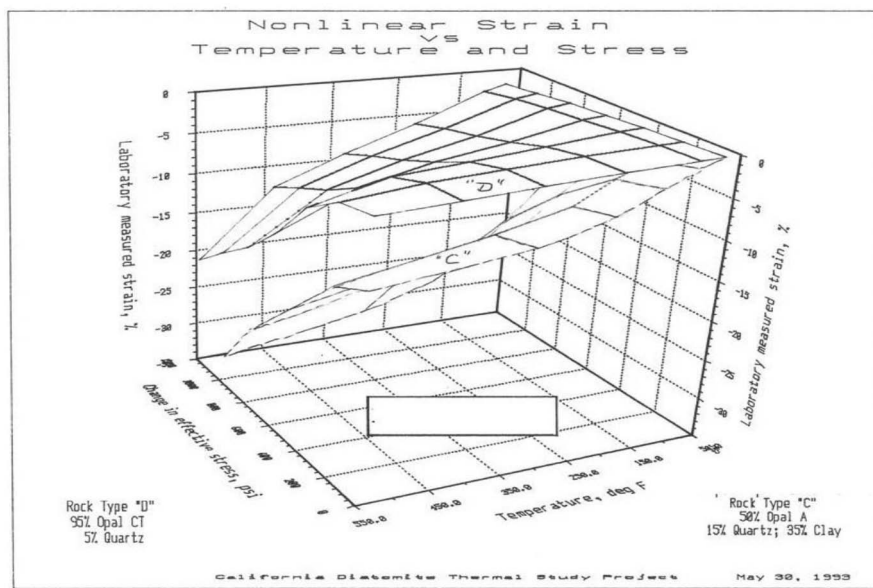


Figure 22—Non-linear strain surfaces versus change in effective stress and temperature measured for Opal-CT and Opal-A rock types

The modeling approach previously shown to be capable of reproducing cyclic steam performance in German and Canadian tar sands (Dietrich 1986) was adopted in this project, whereby the hydraulically induced and propped fractures are modeled as part of the reservoir by use of small-volume, high-transmissibility gridblocks. The ultimate fracture geometry is calculated *a priori* using simple analytical equations and the kinematics of fracture propagation are ignored. The simulator is initialized with the scaled fracture water-filled, and steam is injected at the vertical wellbore. The effective fracture length computed by the simulator is the distance that subtends pore volume penetrated by heat and condensed steam. A stress-dependent absolute permeability function is applied to the fracture gridblocks to reproduce the reported

cycle rates and pressures. More than 850 separate simulation runs were required to obtain the cyclic steam results; most of these runs were necessary to learn how to model the steam injectivity observed in the field. Measured relative permeability data provided good first and final estimates of observed cycle water and oil phase-cuts, without changing the data when modeling both Opal-CT and Opal-A response.

Key mechanisms required to match the observed, initially high cycle oil rates and oil-cuts include thermal expansion of oil (Table 4), counter-current imbibition of water and oil caused by capillary pressure effects, and fracture compressibility. During the cycle injection and soak periods, potential gradients are established which cause the thermally expanded oil to move into the fracture, rather than away from it into the cold, low-permeability diatomite, and oil moves counter-currently into the fracture as steam condensate is imbibed into the water-wet matrix. These same mechanisms have previously been shown to be important when numerically modeling cyclic steam performance (Dietrich 1986).

Steamflood Potential

Flood Patterns

Consideration of the model heating patterns generated by cyclic steaming leads to the well spacing and steamflood pattern design shown in Fig. 23. Viewing the two patterns shown, cyclic steaming of the 8 wells drilled on $\frac{3}{4}$ acre per well spacing would be expected to recover about 7% of the oil originally in-place within the unbounded model area shown with hatch marks. It seems reasonable to express oil recovery efficiency on the basis of the shaded area, because some reservoir volume outside the pattern perimeter was affected by cyclic steaming in the edge producer. The cyclic steam process was shown to be capable of recovering this oil during a 5-year period after 13 cycles, at a CSOR ratio of 4.6 barrels of 1,000 Btu/lb steam per stock tank barrel of oil. Steam slug size was set at 10,000 barrels per cycle; a 3 to 4-month flowback period was assumed with a minimum bottom-hole flowing pressure of 200 psi.

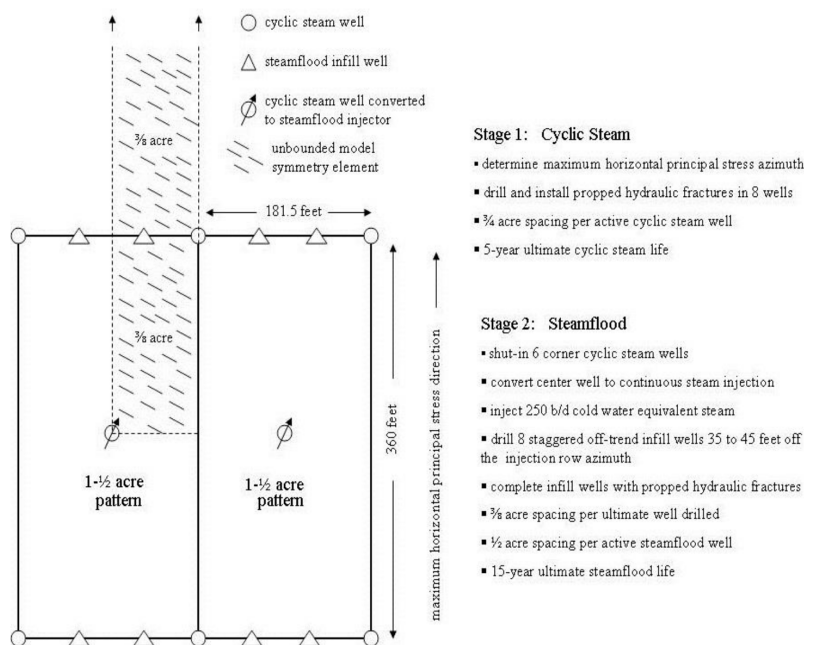


Figure 23—Steam injection pattern layout showing need for ultra-tight well and row spacing

The $\frac{1}{8}$ pattern symmetry element used to predict response to steam injection extends for a distance of 1 mile in a direction parallel to the maximum horizontal principal stress direction; the model was effectively unbounded. Opal-CT reservoir properties were used in the model (Table 1). Once the cycle SOR ratios

approached the economic limit after 5 years of cyclic operations, the center well was converted to continuous steam injection and the corner wells were produced against a bottom-hole flowing pressure of 200 psi. After 5 years of steamflooding without an increase in oil rate, it became obvious that row spacings of 90 feet will be too big, and that infill drilling will be required to steamflood the diatomite.

Oil Bank Buildup

Oil bank buildup in response to continuous steam injection was studied to determine the most attractive locations for infill wells using Opal-CT rock properties and reservoir conditions. Oil saturation is shown in Fig. 24 after 2- $\frac{1}{4}$ years of steamflooding, following 5 years of cyclic steaming (13 cycles) in the center full well and the 4 corner quarter wells. During steamflooding, steam was injected into the center full well located at $x,y = 0,0$. As time goes on, the oil bank and temperature front were shown to move much more rapidly on-trend than off-trend due to permeability anisotropy. Even after 5 years of steamflooding, there was no oil response in the cycled, and therefore pre-heated, corner wells located 90 feet off-trend.

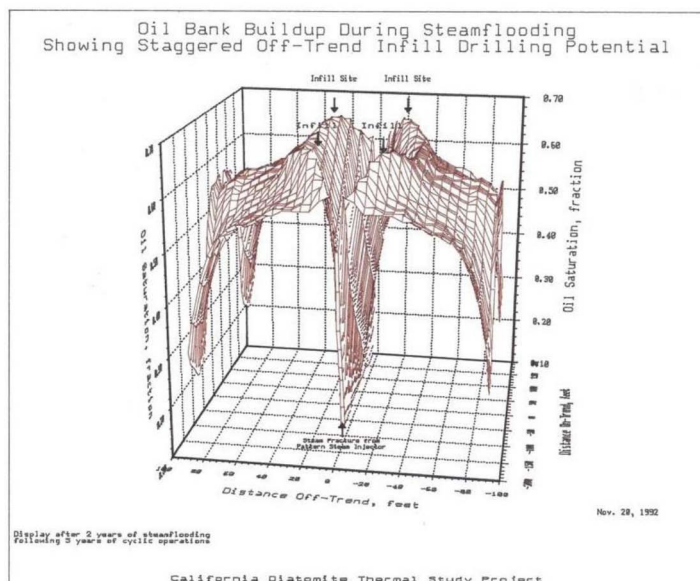


Figure 24—Oil bank build-up during steamflooding showing infill drilling potential 35 to 45 feet off-trend from the injection row

Heating Patterns

Temperature "cones" that develop around the five wells within the 1- $\frac{1}{2}$ acre pattern element after 5 years of cyclic steaming are shown in Fig. 25. In this display, and others to follow, the wells are located at x,y 's of 0,0; 180,90; 180,-90; and -180,-90. More acreage is shown than 1- $\frac{1}{2}$ acres to show the unbounded nature of the pattern element. Fig. 26 shows $\frac{1}{4}$ of the area shown in the prior display. Very little heating is shown in these displays for distances greater than about 35 feet off-trend and 90 feet on-trend. Temperature at each well after the 13th-cycle production period is shown to be about 370°F. This maximum temperature decays to about 185°F at a distance of 37 feet off-trend and about 94 feet on-trend. The "cold" reservoir between the two wells was raised from 115°F at the beginning of cyclic operations to only about 140° to 150° after 13 cycles.

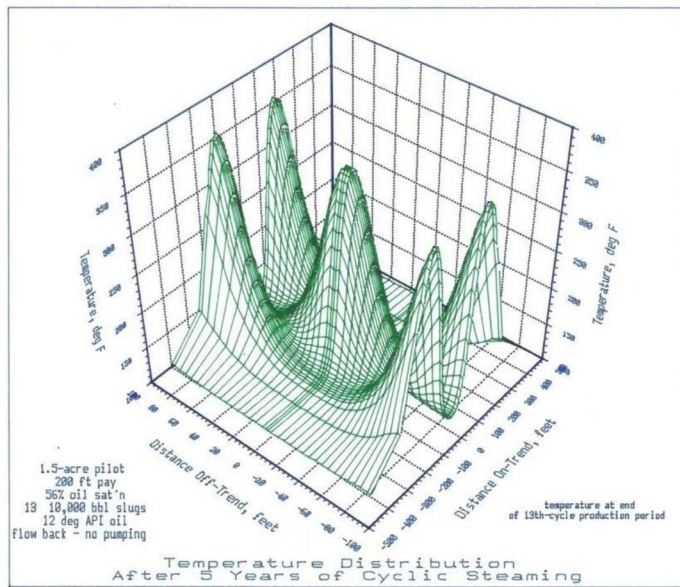


Figure 25—Temperature surface within the 1-1/2 acre pattern element after 5 years of cyclic steaming

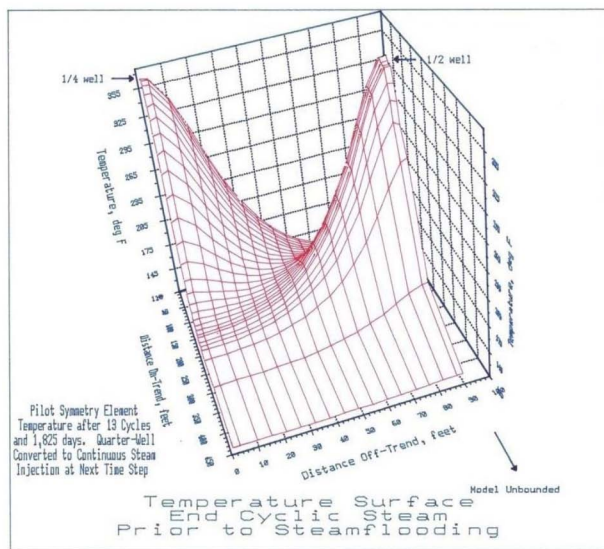


Figure 26—Temperature surface within a quarter of the 1-1/2 acre pattern element after 5 years of cyclic steaming

Two different views of the same temperature conditions after 5 years of steamflooding following the 5 years of cyclic steaming are shown in Figs. 27 and 28. In these displays, we are showing results of a simulation in which an infill well was not drilled. In other words, steam was injected continuously into one previously cycled well (the $\frac{1}{4}$ -well), and only the second previously cycled well drilled on $\frac{3}{4}$ -acre spacing was continuously flowed (the $\frac{1}{2}$ -well). The temperature at the $\frac{1}{2}$ -well located 180 feet on-trend and 90 feet off-trend from the continuous steam injector fell from a level of 370°F at the end of the 13th cycle to about 200°F after 5 years of steamflooding. Figs. 27 and 28 display different views or perspectives of the temperature wave which has moved out from the injector. If an infill well were to be drilled into this temperature "field" at a position of 180 feet on-trend and 26 feet off-trend (Fig. 23), it would encounter a peak temperature of about 225°F .

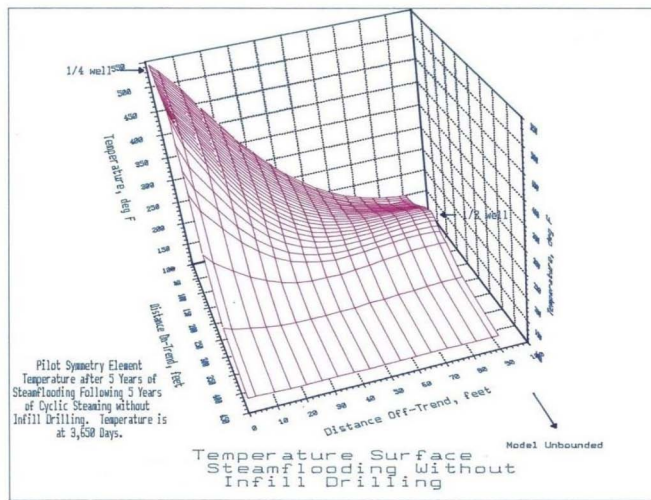


Figure 27—Temperature surface within a quarter of the 1-1/2 acre pattern element after 5 years of steamflooding without Infill drilling and following 5 years of cyclic steaming

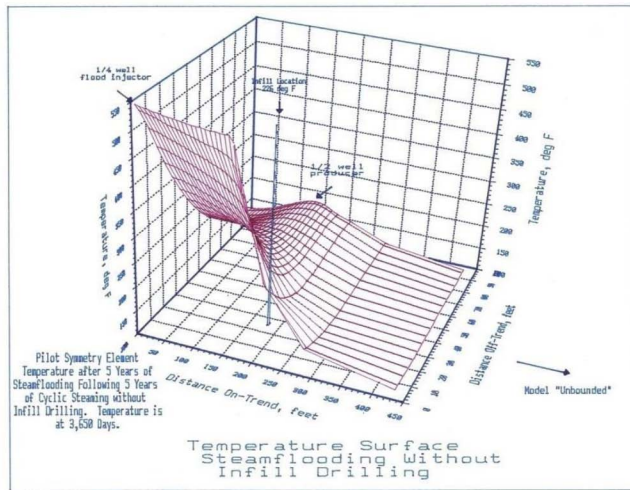


Figure 28—Temperature surface within a quarter of the 1-1/2 acre pattern element after 5 years of steamflooding without infill drilling and following 5 years of cyclic steaming

The temperature distribution reached after 5 years of steamflooding following 5 years of cyclic operations is also shown in Fig. 29. However, in this case numerical results are shown where an infill well was drilled at a location of 180 feet on-trend and 26 feet off-trend after the cyclic operations and at the start of steamflooding. Notice through comparison of Figs. 28 and 29 that, although the $\frac{1}{2}$ -well is still at a temperature of about 200°F , the temperature wave has been pulled much farther on-trend by the infill producing well. A constant injection pressure was used in each of the two simulations, the one with and the one without the infill well. In the case of infill drilling, about 40% more heat was injected into the reservoir after 5 years of steamflooding, and about 50% more heat was produced; the increase in net heat injection was about 35%. The peak temperature encountered by the infill well in this case was 340°F . These model results indicate that an active infill well adds a component of convective heat flow which complements heat conduction.

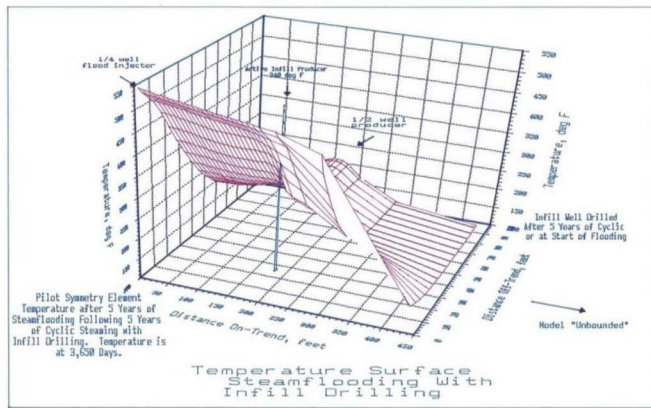


Figure 29—Temperature surface within a quarter of the 1-1/2 acre pattern element after 5 years of steamflooding with infill drilling ana following 5 years of cyclic steaming

Infill Drilling

The most favorable infill locations are found at distances of about 35 to 45 feet off-trend from the injection row azimuth (Fig. 24). Drilling the 8 infill wells shown in Fig. 23 increases the ultimate well density to $\frac{3}{8}$ acre per well; the active well spacing during steamflooding would become $\frac{1}{2}$ acre per well. Staggered infill wells shown in Figs. 23 and 24 are positioned on the basis that injected fluid typically moves away from a diatomite injection well in a direction parallel to the maximum horizontal principal stress direction. Fluid injection is expected to form tensile joints and dilate already existing natural fractures, and these are expected to carry fluid away from the injector in an almost unidirectional manner (parallel to the maximum principal stress direction). Although dilated microfractures and tensile joints will tend to "line-up", many will be subparallel and intersect each other. On the basis of experience with diatomite waterflooding, it is expected that steam and condensate will move oil away from a continuous steam injector in a "bow-tie" pattern (with the injector at the knot in the center), rather than in a circular or ellipsoidal pattern. Hence, the staggered infill well locations are positioned as shown to capture oil displaced during steamflooding.

Potential Oil Recovery

Each infill well was shown to be capable of recovering about 115,000 barrels of oil in response to 310,000 barrels of CWE steam during a 15-year period with the production rate profiles shown in Fig. 30; the CSOR during steamflooding was 2.7 bbl/bbl. Cyclic steaming followed by steamflooding in the manner described was shown to be capable of recovering 42% of the original oil-in-place within the $\frac{3}{4}$ -acre area ($\frac{3}{8}$ -acre within the pattern perimeter and $\frac{3}{8}$ -acre outside the perimeter) shown in Fig. 23. The computed CSOR was 3.0 bbl/bbl.

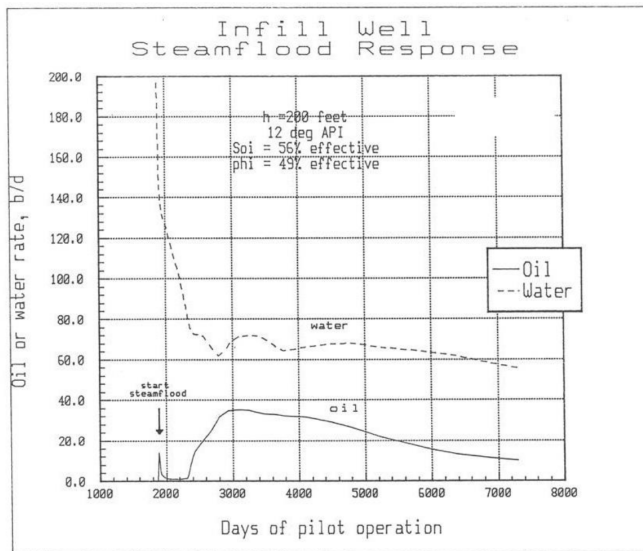


Figure 30—Model infill well oil and water rates in response to continuous steam injection following 5 years of cyclic steaming

Discussion

Opal-A diatomite reservoirs are known to contain much higher concentrations of initial oil-in-place than the levels of 830 to 1300 bbl/ac-ft found at the South Belridge project well. Concentrations have been reported to reach levels of 1800 to 3000 bbl/ac-ft ([Elias and Medizade 2013](#)). In those occurrences, ultimate recovery efficiency and thermal efficiency will be much higher than the levels computed here.

The potential oil recovery and thermal efficiency numbers presented in this paper are based on the ability to achieve good vertical sweep efficiency of diatomite pay intervals with injected steam. The movement of heat and fluids shown here is based on both induced and natural fracture orientations that do not change during the cyclic or continuous injection of steam. At the time of this study, it was not recognized that cyclic steaming or steamflooding using unpropped steam fracs may result in an uncontrolled change in fracture azimuth owing to a change of the in-situ stress regime over time ([Weijers and Wright et al. 1999](#)). Therefore, for the presented results to be meaningful, one must consider that *all* of the cyclic steam or steamflood wells, including the so-called infill wells, may need to be drilled and completed concurrently using *propped hydraulic fractures*. Once in place, the propped fractures would be expected to establish and control essentially unchanging on-trend and off-trend directions of fluid movement, as assumed for the modeling work.

The long term cyclic steam and steamflood potential described here was computed for Opal-CT, a rock type known to compact much less than Opal-A when subjected to increased heat and effective stress. Unlike with Opal-CT, the long term effects of thermally induced compaction of Opal-A include significant loss of permeability and surface subsidence ([Dietrich and Scott 2007](#)). During cyclic steaming operations of Opal-A in the Orcutt field of California, the operator attributes an observed increase in productivity over several *early* steam cycles to dilation of pore throats and/or intense micro-fracturing ([Elias and Wilson et al. 2010](#)). Not surprisingly, the same operator subsequently calculated and reported a decrease in flow capacity for several *later* steam cycles ([Elias and Medizade 2013](#)).

A comprehensive history of the Belridge field development is described by Allan and [Gold et al. \(2010\)](#), where the spacing between rows of longitudinally-fractured horizontal wells has been decreased gradually over time from 75 feet, to 50 feet and finally to 37½ feet. Water injected into these types of wells presumably forms a "wall of water" and a *constant pressure* boundary condition that drives water and oil off-trend. This same ultra-tight, inter-row spacing of 37½ feet was foreseen to be ultimately necessary by operators of both waterflood and steamflood diatomite projects more than 20 years ago, regardless of

whether the "walls of water" or "walls of steam and steam condensate" were considered to be formed by a series of aligned hydraulically induced fractures in vertical wells, or a series of hydraulically induced longitudinal fractures in horizontal wells. The cyclic depositional nature of diatomite establishes multiple stacked intervals (Fig. 1) that in some accumulations are each 50 to 100 feet thick and separated by dense, low permeability sediments. Given this reservoir architecture, staged fracturing using vertical wells in a bottom-to-top sequential completion and flooding scheme *may* be shown to be capable of improving ultimate vertical sweep efficiency as compared to the use of staged longitudinal fractures in horizontal wells.

Conclusions

1. During fluid injection, newly formed microfractures (tensile joints) are most likely to propagate in the rich diatomite layers which contain mostly biogenic silica and little terrigenous material. Floodable net pay may be limited to those intervals in which microfractures or joints propagate.
2. Hydraulic fractures for steamflooding should, to a large extent, parallel the microfractures or tensile joints and the engineer should be aware of a strong permeability anisotropy within the diatomite during fluid injection operations.
3. Operating on bottom-hole pressure control and *without rate constraints*, the thermal simulator was shown to be capable of reproducing the very rapid decline in production rates observed during cyclic steam stimulation of diatomite wells. It was not possible to match the observed response without allowing either a steam-induced or propped hydraulic fracture to close or compress gradually with time during the production period.
4. Commercial success of thermal operations in diatomite will be highly sensitive to the effective oil saturation \times effective porosity product (SoPhi). For the cyclic steam process, a SoPhi product of 0.27 was shown to be capable of delivering a CSOR of 4.1 bbl/bbl for Opal-CT, whereas SoPhi products of 0.15 and 0.23 were shown to yield CSOR values of 7.1 and 3.8 bbl/bbl, respectively, for Opal-A.
5. Increased effective stress and concomitant loss in permeability should be avoided whenever possible by flowing rather than pumping the production wells. Placing a well on pump only once is expected to cause a loss in permeability which can not be regained.
6. Compaction was shown to be unimportant in the cyclic steam process applied to Opal-CT. Energy provided by an expanding steam and hydrocarbon vapor phase was more important than compaction drive, and there was no growth of the compaction "cone" near the well after the initial steam cycle.
7. The spacing between injection and production rows during steamflooding operations will need to be much less than 90 feet. The ultimate well spacing may need to be as low as $\frac{3}{8}$ -acre per well, with the on-trend spacing between vertical injectors about 360 feet and the inter-row spacing between 35 to 45 feet.
8. Given these long-standing conditions of what is now called *ultra-tight* well spacing and effective SoPhi products of 0.27 or greater, oil recovery from an unbounded cyclic steam and steamflood project in Opal-CT may reach 42% of the original oil-in-place within *the floodable net pay*, with a CSOR of 3.0 bbl/bbl.

Acknowledgments

The California Diatomite Thermal Study Project was a private sector consortium research project designed, initiated and directed by The Dietrich Corp. It was undertaken during the period from 1991 to 1993, and co-funded by Arco Oil and Gas Co., Mobil Exploration & Producing U.S. Inc., Texaco USA, and the Unocal Corp. This support is gratefully acknowledged. Mineralogy was determined at the University of California at Santa Barbara; rock mechanics and thermal conductivity/diffusivity at the University of Alberta at Edmonton, Alberta, Canada; heat capacities at Hepler Research and Consulting, Ltd. in Edmonton; residual oil saturation and fluid properties at Hycal Energy Research Laboratories, Ltd., in Calgary, Alberta,

Canada; description of the natural fractures found within the diatomite at Penn State University; and well log analysis at Neal Berry & Associates, Inc. in New Orleans, Louisiana.

Appreciation is extended to Rob Fast, Robert Timmer, Anthony Murer and Tim Ellison, formerly of Mobil Exploration & Producing U.S. Inc., Kent Kuch, formerly of Arco Oil and Gas Co. and Dennis Snow, formerly of Texaco USA for their keen interest and participation in the project. Professor (Emeritus) Don Scott of the University of Alberta, Edmonton was the key researcher for geomechanics and his participation was invaluable. The late Dr. Curtis Chase developed the compaction thermal simulator used in the project while employed at Todd, Dietrich & Chase, Inc.

Nomenclature

| | |
|---------------------|--|
| ϕ_0 | = effective porosity at initial stress and temperature, fraction bulk vol. |
| ϕ | = effective porosity at elevated stress and temperature, fraction bulk vol. |
| k_0 | = absolute liquid permeability at initial stress and temperature, md |
| k | = absolute liquid permeability at elevated stress and temperature, md |
| γ | = dimensionless exponent |
| Black area in track | = bulk volume of oil, fraction |
| one of log plots | |
| CSOR | = cumulative steam / oil ratio adjusted for 1,000 Btu/lb steam, vol/vol |
| CWE | = cold water equivalent |
| ILD | = deep induction resistivity log response, ohm-m |
| MSFL | = microspherically focused resistivity log response, ohm-m |
| PAYFLAG | = net pay = intervals with > 40% total porosity and < 75% total water saturation |
| PHIDGD | = total porosity, or PHID2.65 = total porosity, depending upon the well, fraction bulk vol. |
| PHIE | = effective porosity = difference between total porosity and microporosity, fraction bulk vol. |
| PORECON | = core porosity where measurements made, else PORECON = PHIDGD, fraction bulk vol. |
| SOCORE | = continuous measured oil saturation, fraction pore vol. |
| SOCORECN | = SOCORE where available, else SOCORECN = (1 – SW), fraction pore vol. |
| SOR | = cycle steam / oil ratio, vol./vol. |
| SWE | = effective water saturation, or the water saturation in the effective pore system, fraction pore vol. |
| SXOEPT | = total water saturation, or SW = total water saturation, depending upon the well, fraction pore vol. |
| VOL.TERR | = bulk volume of terrigenous sediments, fraction |
| VOL.OPAL | = bulk volume of biogenic silica, fraction |
| White area in track | = bulk volume of water, fraction |
| one of log plots | |

SI Metric Conversion Factors

| | |
|--------------------|-----------------------|
| bbl × 1.589 783 | E-01 = m ³ |
| Btu × 1.055 056 | E+00 = k j |
| cp × 1.0 | E-03 = Pa.s |
| °F (°F – 32) / 1.8 | = °C |
| ft × 3.048 | E-01 = m |

References

- Allan, M.E., Gold, D.K., and Reese, D.W. 2010. Development of the Belridge Field's Diatomite Reservoirs With Hydraulically Fractured Horizontal Wells: From First Attempts to Current Ultra-Tight Spacing. Paper SPE-133511 presented at the Annual Technical Conference and Exhibition, Florence, Italy. 19-22 September. <http://dx.doi.org/10.2118/133511-MS>.
- Chase, C.A. and Dietrich, J.K. 1989. Compaction Within the South Belridge Diatomite. *SPE Res Eng* **4** (4): 422–428. SPE-17415-PA. <http://dx.doi.org/10.2118/17415-PA>.
- Dietrich, J.K. 2010. The Displacement of Heavy Oil from Diatomite Using Hot Water and Steam. Paper SPE-129705-MS presented at the SPE Improved Oil Recovery Symposium, Tulsa, Oklahoma, 24-28 April. <http://dx.doi.org/10.2118/129705-MS>.
- Dietrich, J.K. and Scott, J.D. 2007. Modeling Thermally Induced Compaction in Diatomite. *SPE J.* **12** (1): 130–144. SPE-97849-PA. <http://dx.doi.org/10.2118/97849-PA>.
- Dietrich, J.K. and Norman, M.R. 2003. Steam Flooding Intensifies Subsidence at Wilmington Field. *Oil & Gas J.* **101**.17 (28 April): 41–50.
- Dietrich, J.K. 1986. Cyclic Steaming of Tar Sands Through Hydraulically Induced Fractures. *SPE Res Eng* **1** (3): 217–229. SPE-11684-PA. <http://dx.doi.org/10.2118/11684-PA>.
- Elias, R., Powell, T. and Medizade, M. 2015. An Analysis of Cyclic Steam Stimulation Projects in the California Opal A Diatomite. Paper SPE-174022-MS presented at the SPE Western Regional Meeting, Garden Grove, California, 27-30 April. <http://dx.doi.org/10.2118/174022-MS>.
- Elias, R. and Medizade, M. 2013. Orcutt Oil Field Thermal Diatomite Case Study: Cyclic Steam Injection in the Careaga Lease, Santa Barbara County, California. Paper SPE-165321-MS presented at the SPE Western Regional & AAPG Pacific Section Meeting, Joint Technical Conference, Monterey, California, 19-25 April. <http://dx.doi.org/10.2118/165321-MS>.
- Elias, R., Wilson, M., Vassilellis, G.D., et al 2010. Successful Thermal Recovery of Heavy Oil From an Ultra Tight Reservoir Renews Development of the 100-Year-Old Orcutt Oil Field. Paper SPE-135520-MS presented at the SPE Annual Technical Conference and Exhibition, Florence, Italy. 19-22 September. <http://dx.doi.org/10.2118/135520-MS>.
- Lorenz, J.C., Warpinski, N.R., Branagan, P.T., et al 1989. Fracture Characteristics and Reservoir Behavior of Stress-Sensitive Fracture Systems in Flat-Lying Lenticular Formations. *J Pet Technol* **41** (6): 615–622; Trans., AIME, 287. SPE-15244-PA. <http://dx.doi.org/10.2118/15244-PA>.
- McGuire, M.D. 1983. Diagenetically Enhanced Entrapment of Hydrocarbons - Southeastern Lost Hills Fractured Shale Pool, Kern County, California. Presented for the Society of Economic Paleontologists and Mineralogists, Pacific Section, Los Angeles.
- Murer, A.S., McClenen, K.L., Ellison, T.K., et al 2000. Steam Injection Project in Heavy-Oil Diatomite. *SPE Res Eng* **3** (1): 2–12. SPE-60853-PA. <http://dx.doi.org/10.2118/60853-PA>.
- Ross, C.M., Vega B., Peng, J., Ikeda, M., Lagasca, J.R.P., Tang, G.-Q. and Kovscek, A.R. 2016. Detecting Opal-CT Formation Resulting From Thermal Recovery Methods in Diatomites. Paper SPE-180369-MS presented at the SPE Western Regional Meeting, Anchorage, Alaska, 23-26 May. <http://dx.doi.org/10.2118/180369-MS>.
- Weijers, L., Wright, C.A., Demetrius, S.L., et al 1999. Fracture Growth and Reorientation in Steam Injection Wells. Paper SPE-54079-MS presented at the International Thermal Operations/Heavy Oil Symposium, Bakersfield, California, 17-19 March. <http://dx.doi.org/10.2118/54079-MS>.

Author

Jim Dietrich is a consulting reservoir engineer with the Dietrich Corporation (TDC) in Pasadena, CA. e-mail: dietrich@cal.berkeley.edu. He previously worked for Shell Oil and Shell Development Companies, where he was involved with thermal recovery and reservoir engineering projects, and Todd, Dietrich & Chase, Inc., where he was a principal and consulting reservoir engineer. Dietrich holds a BA degree in geology and an MSc degree in engineering science from the U. of California, Berkeley.